ACS SENSORS

Open Access
This article is licensed under CC-BY 4.0

pubs.acs.org/acssensors
Article

Electrochemical Vertical Flow Immunoassay for Fast and Decentralized Determination of Stroke-Related Biomarker Glial Fibrillary Acidic Protein

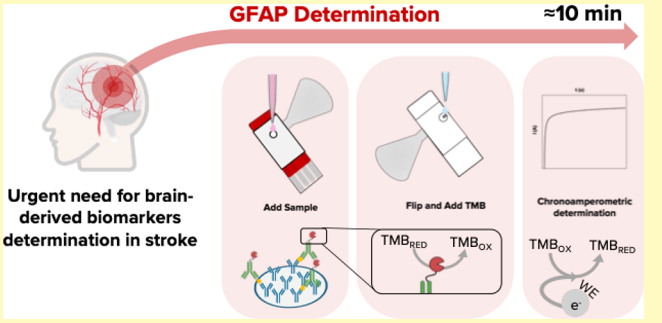
Pablo Rioboó-Legaspi, Cristina Álvarez-Álvarez, Ava Takenaka, Jad Wardeh, Carmen García-Cabo, Lorena Benavente-Fernández, Sergio Calleja-Puerta, Estefanía Costa-Rama,* and M. Teresa Fernández-Abedul*

Cite This: https://doi.org/10.1021/acssensors.6c00801

Read Online

ACCESS | Metrics & More | Article Recommendations | Supporting Information

ABSTRACT: Rapid identification of stroke types remains a major clinical challenge, as current diagnostic methods often rely on neuroimaging, which is time-consuming and not always accessible in pre-hospital settings or remote zones. Glial fibrillary acidic protein (GFAP) has emerged as a promising biomarker for distinguishing hemorrhagic from ischemic stroke, paving the way for rapid, quantitative, and portable detection platforms. Here, we report an electrochemical vertical flow immunoassay (eVFIA) as a point-of-care device for the on-site determination of GFAP. The device combines a multilayer paper-based architecture with a screen-printed electrochemical cell, enabling rapid vertical flow immunoassay and electrochemical signal generation within 10 min. Through systematic optimization of assay parameters, the eVFIA offered a detection limit of 85 pg/mL and strong agreement with standard ELISA measurements. The vertical flow format accelerates fluid transport, while the electrochemical readout ensures quantitative, light-independent measurements. This platform thus offers a cost-effective and user-friendly approach to determine biomarkers for stroke type differentiation. Although further large-scale validation is needed, the GFAP-eVFIA demonstrates strong potential for deployment in decentralized healthcare environments, providing clinicians with a rapid and reliable tool for early stroke assessment.



KEYWORDS: *electrochemical vertical flow immunoassay (eVFIA), GFAP determination, differential diagnosis of stroke, decentralized analysis*

Stroke remains a leading cause of mortality and long-term disability worldwide. Clinically, stroke is primarily classified into ischemic stroke (IS)[1] and intracerebral hemorrhage (ICH),[2] which require different therapeutic approaches. Rapid and reliable differential diagnosis of stroke type is therefore crucial for early intervention and reduced morbidity and mortality.[3]

Current stroke diagnostics rely heavily on magnetic resonance imaging (MRI) and computed tomography (CT) imaging, which require specialized equipment and trained personnel, limiting their accessibility in pre-hospital settings or resource-limited environments. Although there is an increase in the presence of mobile stroke units,[4] which overcome the challenge of on-site diagnosis to some extent, their reach is still limited by high operational costs, limited availability and restricted geographic coverage.

Consequently, the determination of stroke biomarkers has gained attention for rapid and accessible stroke diagnosis. Among them, Glial Fibrillary Acidic Protein (GFAP)[5−7] has been widely studied in different fluids[5,8,9] for differentiating IS from ICH because of its rapid release following ICH, and delayed increase in IS.

Conventional methods for biomarker determination such as ELISA-type immunoassays provide high selectivity and are highly standardized, but remain dependent on centralized laboratories and trained personnel. This limits their suitability for rapid point-of-care (POC) devices[10] that could facilitate quicker stroke classification in remote zones and therefore, improve patient outcome.[11]

Current strategies to decentralize the determination of GFAP have been mostly focused on the use of immunosensors, generally combined with electrochemical transduction. Although these can reach very low limits of detection (e.g., below 0.1 pg/mL[12,13]) and commonly employ a label-free impedimetric approach using screen-printed electrodes, their application still presents some limitations for real-world application, such as complex surface

Received: February 23, 2026
Revised: June 30, 2026
Accepted: July 3, 2026

Downloaded from http://pubs.acs.org/ascefj/article-pdf/doi/10.1021/acssensors.6c00801/6595024z/se-2026-00801z.pdf by guest on 28 July 2026

ACS Publications
© XXXX The Authors. Published by American Chemical Society

https://doi.org/10.1021/acssensors.6c00801
ACS Sens. XXXX, XXX, XXX−XXX

modification protocols and washing steps. Alternative approaches based on the modification of sputtered gold electrodes with molecularly imprinted polymers (MIPs) have also been explored.[14]

Additionally, a fast (*ca.* 15 min) handheld electrochemical GFAP test is commercially available from Abbott, named i-STAT TBI Plasma Cartridge, compatible with the handheld device i-STAT Alinity.[15] This methodology uses a microfluidic dual electrochemical platform to determine both GFAP and Ubiquitin Carboxyterminal Hydrolase L1. However, its high cost (10,000 USD for the i-STAT Alinity and 16 USD for each TBI Plasma Cartridge) still limits its applicability in clinical practice.[16] This unique commercial development demonstrates the enormous interest in brain biomarker information, GFAP included.

Lateral Flow ImmunoAssays (LFIAs) are attractive POC platforms because of their simplicity, low cost and rapid analysis.[17] However, their sensitivity and quantification capabilities are still limited.[18] Electrochemical lateral flow immunoassays (eLFIAs) have therefore emerged to combine the operational advantages of LFIAs with the miniaturization possibilities and sensitivity of electrochemical detection.[19] Nevertheless, integrating a reliable electrochemical cell into LFIAs remains challenging as adequate electrical contact requires sufficient pressure, but excessive compression disrupts fluid flow. Existing strategies, such as integrating SPEs beneath the strip,[20] embedding flat metal electrodes under LFIAs,[21] or printing,[22] or metalizing electrodes[23] directly on the nitrocellulose membrane offer partial solutions, but still suffer from inconsistent contact, low electron-transfer rates and poor reproducibility. For the case of GFAP, the literature is very scarce, with LFIAs developed for GFAP and other traumatic brain injury biomarkers using time-resolved fluorescence,[24] or surface-enhanced Raman spectroscopy,[25] but so far, no simpler eLFIA for GFAP exists.

Vertical flow immunoassays (VFIAs) represent an attractive alternative as perpendicular flow through porous materials enables enhanced interaction times[26] and improves electrical contact with flat electrochemical cells. VFIAs also offer shorter assay times and reduced susceptibility to some limitations observed in lateral-flow systems.[27] Although developments on electrochemical VFIAs (eVFIAs) are still very scarce in the literature, they have demonstrated the potential of the approach for the determination of viral[28] and inflammation[29] biomarkers.

In this work, we introduce a novel eVFIA for the rapid and sensitive detection of GFAP. This device consists of a multilayer microfluidic device, completed with a commercial screen-printed electrochemical cell, modified ad hoc to fit the design of the device. In this eVFIA, the sample is added through the top of the device, leading to the formation of a sandwich immunoassay, where horseradish peroxidase (HRP) is used as a signal amplification label. After this reaction takes place, the device is flipped over to add the substrate of this enzyme, and chronoamperometric determination is performed for quantitative analysis of GFAP. The proposed architecture combines overall vertical flow with lateral flow within each layer of the device, enabling sequential immunoreaction and electrochemical detection without the need to disassemble or manipulate the electrochemical cell during the assay. This is achieved through the integration of a custom-cut SPCE (screen-printed carbon electrode, screen-printed electrochemical cell with carbon as working electrode) and an auxiliary substrate inlet, which allows direct delivery of TMB to the detection zone.

EXPERIMENTAL SECTION

Chemicals

Potassium ferrocyanide, phosphate buffered saline (PBS) tablets, sucrose, and bovine serum albumin (BSA) were purchased from Sigma Aldrich. Sulfuric acid and Tween 20 were provided by Merck. Sodium carbonate and sodium hydrogen carbonate were purchased from VWR. All chemicals were of analytical reagent grade. For all experiments, ultrapure water (dH_2O) purified by a Direct-Q UV 3 purification system (Merck Millipore) was used.

Materials and Fabrication of the Vertical Flow Immunoelectroanalytical Device

For the fabrication of the vertical flow device, the materials used are shown in Table 1.

Whatman CF4, CH1, PROTRAN BA83 and SureWick C083 and G041 were purchased from Sigma-Aldrich. Arcare 8939 was purchased from Adhesives Research. The pressure-sensitive adhesive (PSA) layers were cut via xurography using a cutter-plotter device (Silhouette Portrait 2), designing the corresponding layers with the software Silhouette Studio. The design of the absorbent and substrate pads was drawn onto the corresponding material with an HB pencil using the plotter function. Then, they were cut manually using scissors. The sample pad and nitrocellulose membrane were cut using an 8-mm hole puncher.

The electrochemical cells used were commercial Screen-Printed Carbon Electrodes (SPCEs) from Micrux Technologies (S1PE). These SPCEs (27.5 × 10.1 × 0.35 mm) incorporate three electrodes: a circular (3 mm diameter) working electrode and a hook-shaped counter electrode, both fabricated using carbon ink, along with a silver-ink pseudo-reference electrode. Initially, to create an auxiliary inlet for the device serving as enzymatic substrate pad, a small piece of the electrochemical cell (as shown in Figure S1) was manually cut. After preliminary characterizations, custom-cut electrodes were provided by Micrux Technologies. The eVFIA case was fabricated using a Flashforge Creator 3 3D printer and translucid purple polylactic acid filament (PLA, Flashforge). The patterns were designed on SolidWorks and sliced with FlashPrint5.

To fabricate the device, the electrochemical cell was the basis for placing the different layers of materials. They were assembled from bottom to top following the diagram in Figure 1A. Apart from the electrochemical cell, there are 14 layers, 10 of PSAs and 4 paper-based layers. After placement of each adhesive layer, manual pressure was applied for 10 s. The assembly of one device, starting from already pre-cut materials, can be visualized in the Supplementary Video 1. Devices with suboptimal flow behavior (approx. 3−4% of the devices), attributed to manual misalignment during layer stacking were immediately discarded and their data were not considered for the experiments.

Characterization of the eVFIA: Flow and Electrochemical Measurements

Initial flow studies were performed using food coloring solutions in water. Characterization of the time required for the solution to reach the electrochemical cell was performed using a 5 mM ferrocyanide solution in 10 mM PBS, pH 7.4. After flowing through the different layers, an oxidation signal was produced when this redox probe arrived at the working electrode. Different volumes of this solution were added in the inlet of the device while a chronoamperometric measurement was performed by applying +0.6 V for 600 s to record the oxidation of the electrochemical probe as it flows over the working electrode. Soluble TMB (3,3′,5,5′-tetramethylbenzidine) solution containing H_2O_2 (Abcam, ab210902) was also used to compare the performance of bare and VFIA-integrated SPCE by recording cyclic voltammograms (CVs) of the said solutions.

All electrochemical measurements were performed at room temperature using an μAUTOLAB TYPE III (Metrohm) potentiostat (controlled by NOVA 2.1 program), to which the cell was connected

Downloaded from http://pubs.acs.org/ascefj/article-pdf/doi/10.1021/acssensors.6c00801/6595024z/se-2026-00801z.pdf by guest on 28 July 2026

https://doi.org/10.1021/acssensors.6c00801
ACS Sens. XXXX, XXX, XXX−XXX

Table 1. Materials Evaluated in the Fabrication of the eVFIA Device with Their Corresponding Specifications

material	role in the VFIA	composition	specifications		
			thickness (μm)	capillary flow (mm/s)	pore size (μm)
Whatman CF4	sample pad/pad	cellulose (cotton linter)	482	0.6	20
SureWick C083	sample pad/absorbent pad	cellulose	830	0.67	10
SureWick G041	conjugate pad	glass fiber	410	0.23	1.5
Whatman PROTRAN BA83	nitrocellulose membrane	nitrocellulose	120	0.15	0.2
Whatman CH1	substrate pad	cellulose	180	0.72	11
ARcare 8939	flow control and structural support	polyester film coated with vinyl adhesive	126	NA	NA

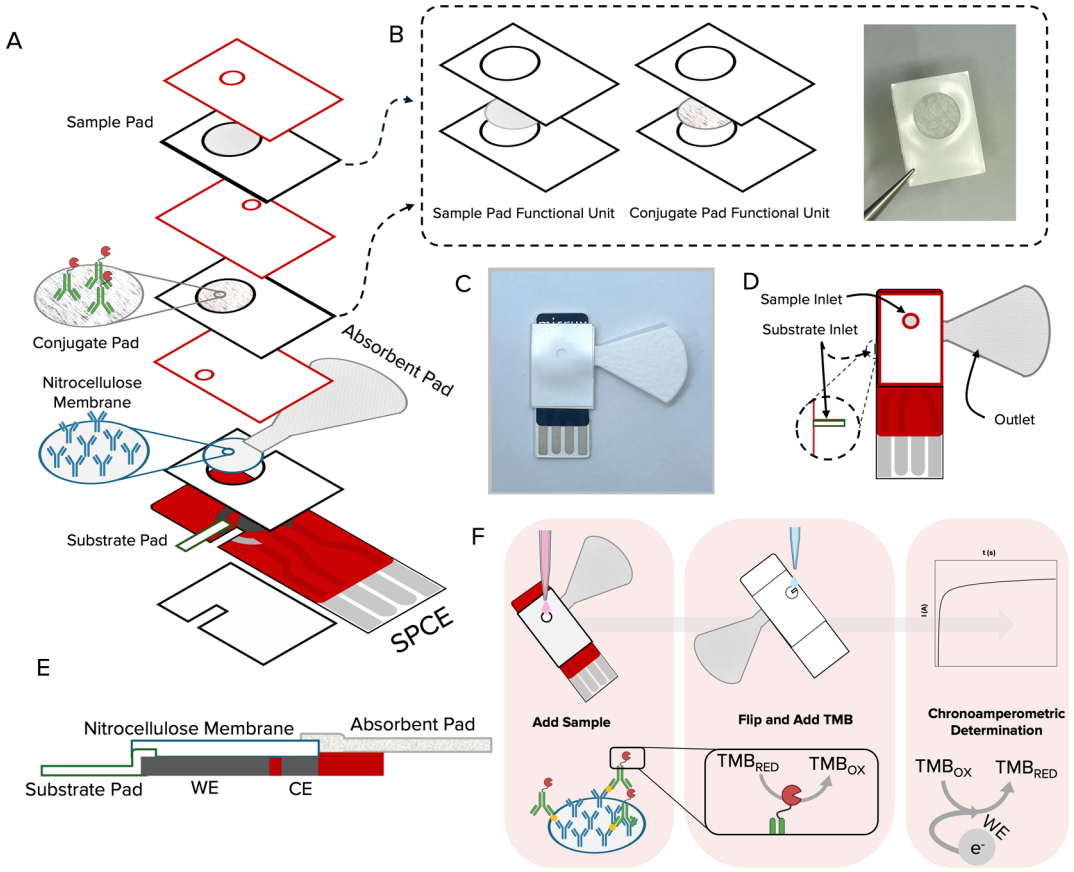


Figure 1. Design of the eVFIA device. (A) Multilayer design of the device. Pressure sensitive adhesive layers (PSA) are indicated as white pieces with both red (flow control) and black (structural) outer lines. Paper layers are indicated with their names. SPCE: Screen-printed carbon electrode. (B) Detail on sample and conjugate structural units. (Right) Picture of a sample structural unit. (C) Picture of the device once fabricated. (D) Schematic representation of the main inlet, auxiliary inlet (dashed circle, detail of the back of the device) and outlet. (E) Transversal detail of the device along the custom-cut slit, with detail on the arrangement of the substrate pad, nitrocellulose membrane, SPCE, and absorbent pad. (F) Workflow of the eVFIA assay. (Top) Steps to be performed in the eVFIA device. (Bottom) Immunoassay scheme with the enzymatic oxidation of the TMB substrate and its subsequent electrochemical reduction for GFAP quantification.

using a SPE-Box connector (Micrux Technologies). For the decentralized setup, a Micrux ECSens portable potentiostat (controlled by EC Manager app) was used.

GFAP Sandwich Enzyme Immunoassay

The antibodies (Abs) employed in the immunoassay performed, either using the eVFIA or an ELISA plate with colorimetric readout, were all purchased from Abcam. The pair of antibodies consisted of a capture anti-GFAP Ab (ab222279) and a recombinant HRP-labeled anti-GFAP Ab (ab305709) as detection antibody. GFAP standard (ab114149) was also provided by Abcam. All plate-based immunoassays were performed on microtiter plates (ab210903). As enzymatic substrate, TMB solution (ab210902) was used. The buffers used for plate-based ELISA were the coating buffer (CB, 35 mM NaH_2CO_3, 15 mM Na_2HCO_3, pH 9.6), blocking buffer (BB, 0.5% Tween 20 with 1% BSA in 10 mM PBS, pH 7.4), and washing buffer (WB, 0.5% Tween 20 in 10 mM PBS, pH 7.4). Shortly, plates were coated with the corresponding capture Ab at 2 μg/mL in CB for 2 h. After washing, the wells were blocked with 300 μL of BB overnight at 4 °C. The wells were washed, and the corresponding standard GFAP solution (prepared by dilution in BB) was added and maintained for 2 h. After that, the plate was washed and the corresponding detection Ab solution was added at a concentration of 0.5 μg/mL in

https://doi.org/10.1021/acssensors.6c00801
ACS Sens. XXXX, XXX, XXX−XXX

Downloaded from http://pubs.acs.org/ascefj/article-pdf/doi/10.1021/acssensors.6c00801/65950242/se-2026-00801z.pdf by guest on 28 July 2026

BB. After the incubation of the detection Ab for 2 h, plates were washed and 100 μL of TMB solution was added and incubated in the dark for 20 min. Then, 100 μL of 1 M H_2SO_4 was added to stop the reaction. Absorbance was read at 450 nm using an Eon plate reader. All the incubation steps were performed adding volumes of 50 μL, in an orbital shaker (MSC-100, Allsheng Instruments) at 400 RPM at room temperature if not indicated otherwise. All washes were performed three times with 350 μL of WB.

eVFIA Assay

To integrate the immunoassay into the eVFIA device, a protocol modified from a lateral flow immunoassay was developed.[30] Thus, the three functional papers were treated adequately as follows. The sample pad was submerged in a sample pad buffer (1× PBS, 0.5% BSA, 0.05% Tween 20) and then dried for at least 2 h at 37°C. For the conjugate pad, 25 μL of HRP-labeled detection Ab solution prepared in the corresponding concentration in the conjugate pad buffer (10 mM PBS, 1% BSA, 0.05% Tween 20 and 5% sucrose, pH 7.4), were deposited on the conjugate pad and dried for at least 2 h at 37 °C. To prepare the nitrocellulose membrane, 1 μL of the corresponding concentration of capture Ab solution (in 10 mM PBS, pH 7.4) was added to the center of the membrane. Then, it was dried for 10 min at RT. After that, the membranes were blocked by completely covering them with Membrane Blocking Buffer (10 mM PBS, 2% BSA, pH 7.4) and incubating them for 20 min at room temperature with gentle shaking (200 RPM) in an orbital shaker. After that, the membranes were washed three times with Membrane Washing Buffer (10 mM PBS, 0.05% Tween20, pH 7.4) for 15 min at room temperature with gentle shaking. Finally, membranes were dried for at least 2 h at 37 °C. Absorbent and substrate pads did not require any specific modification.

After preparing the paper layers, eVFIA devices were carefully assembled to integrate the quantitative electrochemical detection and the enzymatic immunoassay. For assaying the device, an appropriate volume of the sample or standard was added to the main inlet of the device. After 5 min, the device was flipped and 50 μL of TMB solution were added through the auxiliary inlet. After 5 additional minutes, chronoamperometric measurements were performed applying a potential of 0.0 V for 30 s. The average current measured between 25 and 26 s, at a time when the amperometric response was considerably stabilized, constituted the analytical signal.

Real Sample Analysis

Serum samples of stroke patients were collected in the stroke unit of the Hospital Universitario Central de Asturias (HUCA). All patients were over 18 years of age and signed an informed consent. The procedures adhered to the tenets of the Declaration of Helsinki on biomedical research involving human subjects. Full ethical approval was obtained from the Research Ethics Committee of the Principality of Asturias (Oviedo, Spain) (CEImPA No. 2024.016). Samples were 1:10 diluted in 10 mM PBS 7.4 before measurement by eVFIA device and ELISA in microtiter plate if the analytical signal exceeded that of the highest value of the linear range.

■ RESULTS AND DISCUSSION

Design of the Electrochemical Vertical Flow Assay (eVFIA) Device

The immunoassay used to design the GFAP-eVFIA follows a sandwich format, in which GFAP (analyte) first binds to the HRP-detection Ab to form a detection antibody-analyte complex that is subsequently captured by the immobilized capture Ab. Thus, the analytical signal results from the electrochemical reduction of TMB that has been previously oxidized by the enzyme HRP.

To enable sequential delivery and interaction of all reagents, several paper components are required: a sample pad for loading and conditioning the sample, a conjugate pad containing the HRP-detection Ab, a nitrocellulose membrane where the capture Ab is immobilized, and a substrate pad for TMB solution delivery. The design of the device can be observed in Figure 1A. The main difference in the design of this eVFIA when compared to the common immunochromatographic assays is that the electrochemical cell is the basis of the device, this being the component that provides quantitative results. In this case, the design relies on overlaying the different functional layers on top of each other, while incorporating different PSA layers between the paper layers, some with the purpose of giving mechanical support (structural PSA) and others used to control flow rate and direction (flow PSA). Starting from top to bottom, a main inlet can be found, where the sample is added so it would flow into the sample pad. In this layer, the top PSA liner is not removed to provide a hydrophobic surface so that the sample goes directly into the inlet. Both the sample and conjugate pads are enclosed in structural PSA layers to form functional units with mechanical support (Figure 1B).

Since ideally the sample should flow in a slow and controlled manner, a flow PSA layer with a small side circular inlet was added after each functional unit. The nitrocellulose membrane is supported on top of the SPCE with an additional PSA. Next to the nitrocellulose, a fan-shaped absorbent pad is placed as the driving paper microfluidic force, with a ∼2 mm superposition over the nitrocellulose membrane, as its progressively expanding wicking area lowers flow resistance during liquid advance and sustains faster capillary transport than a constant-width pad.[31] This absorbent initially ended on a wider square shape (as shown in Figure 2B) but was later changed to the final round-edge configuration, providing equivalent performance with less fragility after liquid solutions flow through the material. Within the SPCE, an auxiliary inlet strip is placed on a custom-cut slit between the auxiliary and pseudo-reference electrodes. This inlet strip allows direct flow of substrate solution into the nitrocellulose membrane. Lastly, a backing PSA is added for support. The complete fabricated device is shown in Figure 1C and detailed dimensions of the layers are shown in Figure S2.

This device, once fabricated, presents a main inlet, an auxiliary inlet (for enzymatic substrate addition), and an outlet, as shown in Figure 1D. Each layer of the device covers a specific purpose, giving the device structure and providing an optimized flow between layers. The flow control PSAs after each functional unit ensure a vertical flow between layers, but horizontal (or lateral) within each layer, favoring the interaction of the analyte in the sample with the immobilized immunoreagents, in both the conjugate pad and nitrocellulose membrane. The substrate inlet allows direct flow of enzymatic substrate into the nitrocellulose membrane once the sandwich immunocomplex was formed. This integrated configuration constitutes one of the key advantages of the proposed design, as it combines lateral flow within individual paper layers with overall vertical transport through the device, while enabling substrate addition directly through the integrated SPCE without requiring electrode disassembly or external transfer steps. The possibility of custom-cutting the polymeric SPCE substrate facilitated incorporation of the auxiliary inlet into the multilayer architecture.

Additionally, the absorbent pad is in contact with the nitrocellulose membrane on its top, not only to prevent breaking

Downloaded from http://pubs.acs.org/ascefj/article-pdf/doi/10.1021/acssensors.6c00801/6595024z/se-2026-00801z.pdf by guest on 28 July 2026

https://doi.org/10.1021/acssensors.6c00801
ACS Sens. XXXX, XXX, XXX−XXX

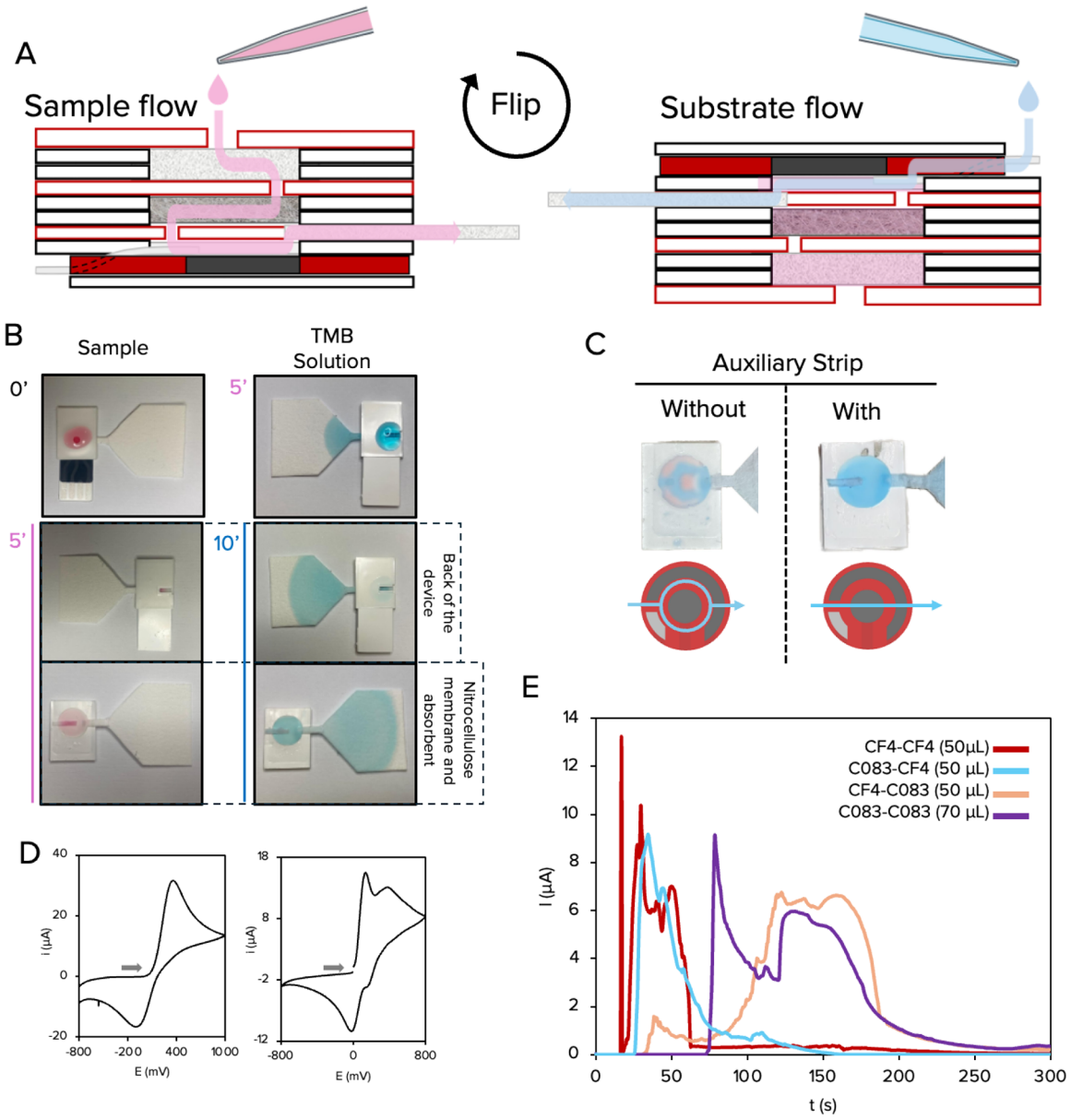


Figure 2. Flow characterization of the eVFIA device. (A) Scheme of the flow in the proposed device. (Left) Flow of the sample to be tested, in pink. (Right) Flow of the TMB substrate once the device is flipped, in blue. (B) Flow evaluation of the device using colored solutions. (Left) Sample flow evaluation; a sample is simulated by using water dyed with red food coloring. (Right) TMB solution flow evaluation. TMB solution is simulated by using water dyed with blue food coloring. (C) Evaluation of the use of the auxiliary inlet strip. (Top) Pictures of nitrocellulose membrane after adding the simulated sample and TMB solutions. (Bottom) Scheme showing the preferential direction of simulated TMB solution for both designs. (D) CVs recorded at 0.1 V/s in the eVFIA device after adding 50 μL of a 5 mM potassium ferrocyanide solution (left) or TMB solution (right) and waiting for 5 min. (E) Evaluation of different combinations of the thin (Whatman CF4) and thick (SureWick C083) cellulosic materials used as sample and absorbent pads. Chronoamperometry performed at +0.6 V using 5 mM potassium ferrocyanide solution for the different combinations of materials tested. Legend shows the combination of sample-absorbent pad and the volume of ferrocyanide solution tested, in brackets.

this fragile material but also to ensure that the sample and substrate solution pass through the membrane, where capture antibodies are immobilized and sandwich reaction will occur (Figure 1E).

The general workflow of this eVFIA is schematically shown in Figure 1F. The sample to be determined is added to the top of the device, from where it flows through the different layers, while the analyte (GFAP) selectively interacts with the corresponding immunoreagents (first with the HRP-detection Ab and then with the capture Ab). Thus, an HRP-labeled sandwich immunoconjugate would form over the nitrocellulose membrane. Then, the enzymatic substrate solution (TMB/H_2O_2) is added through the substrate pad and consequently, TMB is enzymatically oxidized. Finally, this oxidized TMB is electrochemically reduced by chronoamperometry at an adequate potential, producing a cathodic current that is proportional to the concentration of GFAP in the sample. The cut made in the polymeric screen-printed cell between the auxiliary and reference electrodes to add the substrate from the backside, prevents its reaction with the enzymatically conjugated

https://doi.org/10.1021/acssensors.6c00801
ACS Sens. XXXX, XXX, XXX−XXX

Downloaded from http://pubs.acs.org/ascefj/article-pdf/doi/10.1021/acssensors.6c00801/65950242/se-2026-00801z.pdf by guest on 28 July 2026

antibodies that remain in the flow path, leading the substrate directly toward the working electrode.

Flow Performance Characterization and Optimization

Starting from this design, the flow characteristics of the device were tested to ensure that both the sample and the TMB substrate solutions flow adequately within the device. Figure 2A shows the flow route of both, depicting how the general flow is vertical, but horizontal in each individual paper layer. One of the advantages of the mixed vertical/lateral flow model is that, although the nitrocellulose membrane is attached to the electrochemical cell by a ring of adhesive layer, the weight of the rest of materials on top, as well as that of the solutions, that also enter from the top, must be considered. In contrast, in a single lateral flow model, the weight supported by the electrodes is only that of a thin layer, and thus the contact could be more inconsistent.

Figure 2B pictures the flow of these solutions within the device using colored simulated solutions. Firstly, 50 μL of a red water-based food coloring in water, used as a simulated sample solution, were added to the main inlet of the device. After 5 min, the nitrocellulose membrane can be seen dyed red from the back of the auxiliary strip, which is confirmed after removing the SPCE from the device (Figure 2B, left, 5′ box). Furthermore, if 50 μL of a simulated TMB solution (blue water-based food coloring in water) is added to a simulated sample-loaded device, it can be seen that the solution easily flows toward the absorbent pad and when the SPCE is removed after 5 min, the nitrocellulose can be seen completely dyed blue, indicating the drainage of the simulated sample toward the absorbent pad (Figure 2B, right, 10′ box). This is an essential requisite as this is where the immunoassay would take place. Not only is it crucial for the TMB solution to be in contact with the immunoenzymatic conjugate, but also for the removal of the sample matrix, as this would also contain the excess of immunoreagents, preventing unwanted interactions or background signal.

Additionally, the need for a strip in the auxiliary inlet was assessed, as initially the TMB solution could be directly dropped on the back of the nitrocellulose membrane through the custom-cut slit. For this, devices with and without the auxiliary strip were fabricated, and 50 μL of the simulated sample solution were added from the inlet of the device. After 5 min, 50 μL of a simulated TMB solution were added from either the back of the nitrocellulose or the auxiliary strip, respectively. As can be seen in Figure 2C, the device without auxiliary strip shows no blue color on the center of the nitrocellulose membrane, while the one with the auxiliary strip shows a homogeneous blue color. When looking closely at the surface of the screen-printed electrodes, fabricated using thick-film technology with layer thicknesses in the μm-scale, it can be observed that the carbon/silver inks and the dielectric material create ridges, making a more favorable flow through the zones of the nitrocellulose contacting dielectric material as it has a height similar to that of the absorbent pad (as shown in Figure 1E). For this purpose, an inlet strip that adds the TMB directly from below ensures TMB solution covers the whole nitrocellulose area and leaves the device through the absorbent pad.

Even though the device is based on a commercial SPCE, it was evaluated whether the characteristic oxidation and reduction processes of both potassium ferrocyanide, a well-known redox probe, and TMB could be recorded on the eVFIA. Figure 2D shows CVs recorded in 5 mM ferrocyanide and in TMB solutions with the eVFIA device. The measures were performed after 5 min of the addition of the solutions (the former through the sample inlet and the latter through the substrate inlet), to ensure complete permeation of the solution through the multilayer structure and full wetting of the electrode surface prior to measurement. Since the solution becomes quiescent, well-defined processes are obtained. These CVs present the expected electrochemical behavior of both species, showing the characteristic oxidation and reduction processes of ferrocyanide (at +336 and −96 mV, respectively), and the two oxidation and reduction processes of TMB in neutral pH (at +157 and +408 mV and +168 and +5 mV, respectively).

Finally, two cellulose-based materials, Whatman CF4 and SureWick C083, were evaluated as sample and absorbent pads based on their flow characteristics. Both materials are suitable for either role, as reported in previous LFA studies,[32,33] and exhibit similar nominal capillary flow rates (0.6 vs 0.67 mm/s). However, CF4 presents larger pores (20 vs 10 μm) and lower thickness (482 vs 830 μm), which is expected to reduce flow resistance and promote faster but less sustained wicking,[34,35] whereas C083 supports higher fluid retention and more prolonged transport due to its smaller pores and greater thickness.[36] These principles align with the Washburn-type behavior of cellulose networks, where pore geometry dictates capillary suction and thicker matrices prolong fluid residence. Thus, despite similar nominal capillary flow rates, CF4 and C083 are expected to generate fast-transient and slow-sustained flow profiles, respectively.

To evaluate their influence on fluid transport, devices with different pad combinations were tested by chronoamperometry with a 5 mM potassium ferrocyanide solution added to the inlet. The oxidation current was used as a proxy for fluid arrival and establishment of ionic contact between electrodes. As shown in Figure 2E, devices incorporating CF4 absorbent pads exhibited rapid, spike-like current responses, indicating fast fluid transport, with the sample reaching the electrodes in less than 30 s and relatively short residence times (45 s for CF4−CF4 combinations and 110 s when paired with C083 as sample pad, calculated as the time between the increase in the current and its return to the baseline). When using a lower volume (40 μL), no current was observed (Figure S3, inset), suggesting insufficient fluid contact with the electrodes.

In contrast, devices containing C083 as absorbent pad showed a more gradual and sustained current response, reflecting slower fluid uptake and extended interaction within the detection zone. In these configurations, residence times exceeded 200 s, reaching 265 s for the CF4−C083 combination and 225 s for the C083−C083 configuration. This behavior suggests a better balance between fluid delivery and retention, allowing prolonged contact between the solution and the electrochemical interface. Interestingly, when using smaller volumes (Figure S3, orange and purple curves) a behavior similar to that of the CF4 absorbent is observed, which is consistent with capillary-driven systems where insufficient input volume prevents full saturation of the nitrocellulose and limits the establishment of a sustained flow between layers.[37]

Overall, these results demonstrate that fluid transport in the device is governed by the interplay between pore size, fiber packing, and absorbent capacity rather than nominal capillary rate alone.[35] Thicker pads sustain capillary action over longer

Downloaded from http://pubs.acs.org/ascefj/article-pdf/doi/10.1021/acssensors.6c00801/6595024z/se-2026-00801z.pdf by guest on 28 July 2026

https://doi.org/10.1021/acssensors.6c00801
ACS Sens. XXXX, XXX, XXX−XXX

periods due to their higher absorbent volume, especially when paired with materials of complementary porosity.[37] The CF4−C083 configuration, along with a sample volume of 50 μL, provides the most favorable compromise between rapid sample delivery and sustained residence time, enabling efficient signal generation with minimal sample volume.

Integration of the Immunoassay with the eVFIA Device

Prior to achieving a full quantitative performance, several aspects of the integration of the GFAP immunoassay into the eVFIA device were optimized. Initially, the combination of immunoreagents, purchased separately and not provided as a pre-assembled kit, was tested in a conventional plate-based immunoassay to ensure an appropriate interaction (Figure S4), obtaining great linearity in the GFAP concentration range indicated by the provider (50−5000 pg/mL, R^2 = 0.997). Then, the concentration of the capture Ab in the nitrocellulose membrane (Figure 3A, left) and the HRP-labeled detection Ab on the conjugate pad (Figure 3A, right) were optimized by assaying different concentrations for 0 ng/mL (blank) and 1 ng/mL (signal) of GFAP. The best signal/blank ratio was achieved with concentrations of 100 and 5 μg/mL for capture and detection Ab, respectively. Furthermore, the times for sample incubation (Figure 3B, left) and TMB substrate reaction (Figure 3B, center) were univariately optimized, by varying each step duration, while keeping the other constant (starting from a value of 5 min). Based on previous flow optimization, all volumes were fixed to 50 μL. The best response was achieved for 5 min. This leaves

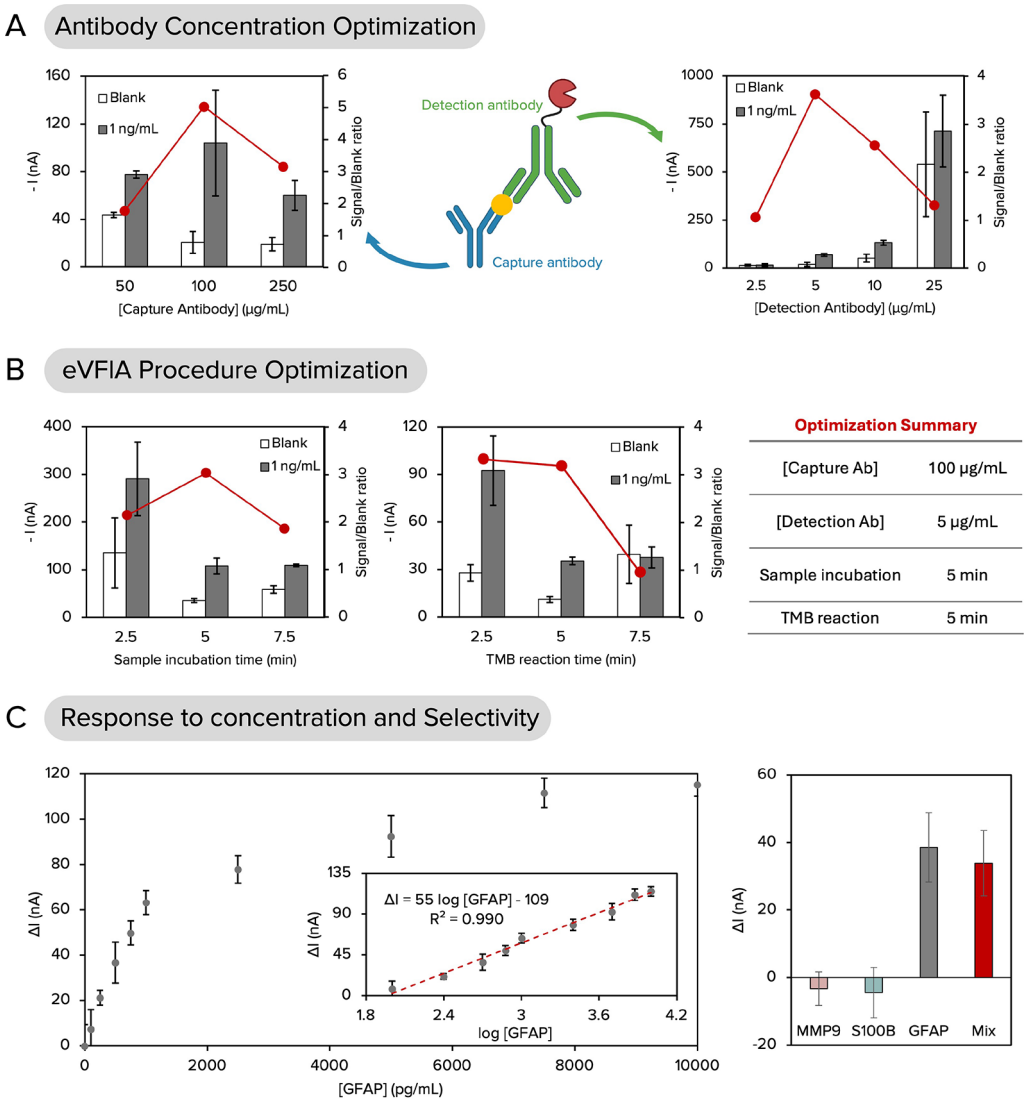


Figure 3. Integration of the GFAP immunoassay into the eVFIA device. (A, B) Immunoassay optimizations. (A) Optimization of the concentration of de Capture (left, [Detection Antibody] = 10 μg/mL) and detection (right, [Capture Antibody] = 100 μg/mL) Ab (sample and TMB incubation time = 5 min each, for both experiments). A schematic with the sandwich immunocomplex is shown at the center. (B) Optimization of the sample incubation time (left, TMB incubation time = 5 min) and TMB reaction time (center) using the previously optimized conditions. A summary with the optimization results is shown at the right. For each optimization a blank (0 ng/mL) and a 1 ng/mL GFAP solution were used. Results are given in terms of the cathodic current intensity measured by chronoamperometry at 0 V at 30 s (white and gray bars, left axis), and the corresponding signal/blank ratio for each condition (red dataset, right axis). (C, left) Calibration curve obtained with the GFAP-eVFIA device under optimized conditions. Inset: logarithmic fitting of the calibration curve. (Right) Selectivity study performed using MMP9 (100 ng/mL), S100B (0.1 ng/mL), GFAP (0.5 ng/mL), and a mix of the three proteins under the same optimized conditions.

Downloaded from http://pubs.acs.org/ascefj/article-pdf/doi/10.1021/acssensors.6c00801/65950242/se-2026-00801z.pdf by guest on 28 July 2026

https://doi.org/10.1021/acssensors.6c00801
ACS Sens. XXXX, XXX, XXX−XXX

the full reaction time (without electrochemical determination) in 10 min, and a full analysis time of 10 min and 30 s. A summary of the optimized conditions is displayed in the table of Figure 3B.

It should be considered that some materials included in the design could favor nonspecific binding (NSB). In this case, however, the PSA layers employed were specifically selected because they are commonly used in microfluidic device fabrication. In the proposed architecture, these layers: (i) Provide structural and mechanical support to the multilayer paper-based assembly. Each functional circular paper-based pad is supported by a PSA layer, which has a circular cutout approximately matching the pad diameter. Therefore, the contact area between these PSA layers and the solutions is negligible, as should NSB. (ii) Define and control the vertical flow path within the device. Although the main immunochromatographic flow and bio/chemical interactions occur through the cellulose/glass fiber/nitrocellulose-based porous materials, limited contact between the outer region of the porous pad and the PSA layers may occur. However, possible NSB phenomena are monitored through blank measurements. Moreover, the addition of the substrate solution through the back of the device, directs it toward the working electrode minimizing its interaction with the main flow path.

Using the optimized conditions, a calibration curve was obtained over a dynamic range comprised between 0.1 and 10 ng/mL, showing high linearity when the increase in cathodic current (ΔI, calculated as the difference between the measured cathodic current with GFAP, and the blank signal recorded by chronoamperometry), is represented against the log of the GFAP concentration (Figure 3E). A limit of detection (LOD) of 85 pg/mL, calculated as the concentration corresponding to a signal that is 3 times the standard deviation of the estimate in the first order of concentration, was obtained. The linear range obtained overlaps with the concentrations typically observed in moderate-to-severe stroke cases, particularly in the early hours after symptom onset, where serum GFAP levels frequently reach the ng/mL range. Reported clinical concentrations span approximately from 0.1 to 100 ng/mL.[5,9,38,39] Therefore, the working range of the proposed eVFIA covers the concentration interval relevant for distinguishing pathological GFAP elevations from baseline physiological levels, supporting its potential applicability for stroke triage and decentralized point-of-care testing.

Finally, the selectivity of the proposed eVFIA was evaluated in the presence of potentially interfering biomarkers relevant to stroke and neurological disorders, specifically matrix metalloproteinase-9 (MMP9) and S100 calcium-binding protein B (S100B), as these are commonly associated with acute brain injury and may coexist with GFAP in serum samples from stroke patients. Interference studies were performed using concentrations representative of pathological levels reported in neurological disorders (100 ng/mL for MMP9[40] and 0.1 ng/mL for S100B[41]), together with 0.5 ng/mL GFAP. As shown in Figure 3C (Right), the ΔI values obtained for MMP9 and S100B alone showed values close to zero, with no significant differences observed between them ($p = 0.88$). In contrast, samples containing GFAP produced the analytical response in agreement with the calibration curve. The GFAP signal was not significantly affected in the presence of the interfering biomarkers (GFAP vs GFAP + MMP9 + S100B, $p = 0.51$). Both GFAP alone and in the presence of the interferents showed a statistically significant difference when compared with MMP9 ($p = 0.002$ and 0.004, respectively) and S100B ($p = 0.006$ and 0.004, respectively) alone. These results confirm the selectivity of the proposed immunoassay toward GFAP under the evaluated experimental conditions.

GFAP eVFIA Performance Validation

To assess the clinical relevance of the GFAP eVFIA, and as a proof-of-concept, four human serum samples from stroke patients were analyzed and compared to a conventional plate-based ELISA (Table 2), considering a 1:10 dilution in the sample if the analytical signal exceeded that of the highest point of the calibration curve. Student's *t*-test demonstrated agreement between the results obtained with both methods, as all the *p*-values were above 0.05, showing statistical concordance between the methods.

Nevertheless, some limitations should be acknowledged. The present validation was performed with a limited number of clinical samples, and broader studies are required to establish diagnostic accuracy across diverse patient populations and stroke severities. Additionally, while the assay demonstrated statistical correlation with ELISA, recovery at lower concentration ranges requires further optimization to ensure consistent quantitative performance. Device robustness and reproducibility under real-world conditions, including variable sample matrices and operator handling, also remain to be fully evaluated.

Toward a Decentralized and User-Friendly Device

To further support decentralized diagnostic workflows, a custom housing for the eVFIA was designed to enable secure integration of the device (Figure 4A). This casing presents an inlet for the sample, as well as an inlet for the enzymatic substrate on the back. After inserting the eVFIA device through the top of the case, a sliding part is fixed to secure the device. The connections of the SPCE protrude from the bottom of the case for its connection with the potentiostat. The casing is an interface that ensures proper alignment for sample addition, mechanical stability, and prevents contamination or wrong handling, helping the device to be used reliably outside laboratory environments.

Furthermore, the compatibility of the eVFIA in its casing with a commercially available USB-C portable potentiostat was assessed (Figure 4B), observing that the TMB solution signal recorded by CV presented the expected oxidation and reduction peaks, confirming consistent signal acquisition with different types of potentiostats. This configuration facilitates deployment in point-of-care and field-based settings, where access to benchtop instrumentation is limited such as schools, community health centers, mobile health units, and remote research stations. This decentralization is particularly relevant

Table 2. Real Sample Analysis[a]

sample	eVFIA [GFAP] (ng/mL)	ELISA [GFAP] (ng/mL)	*p*-value
1	0.16 ± 0.09	0.28 ± 0.02	0.092
2	10.1 ± 0.9	12.2 ± 0.2	0.056
3	5 ± 1	4.74 ± 0.04	0.75
4	1.9 ± 0.5	1.6 ± 0.2	0.35

[a]For each sample, the concentration of the serum sample obtained with the GFAP eVFIA and the plate-based GFAP ELISA are given *p*-values for paired Student's t-test are given for each sample.

Downloaded from http://pubs.acs.org/ascefj/article-pdf/doi/10.1021/acssensors.6c00801/65950242/se-2026-00801z.pdf by guest on 28 July 2026

https://doi.org/10.1021/acssensors.6c00801
ACS Sens. XXXX, XXX, XXX–XXX

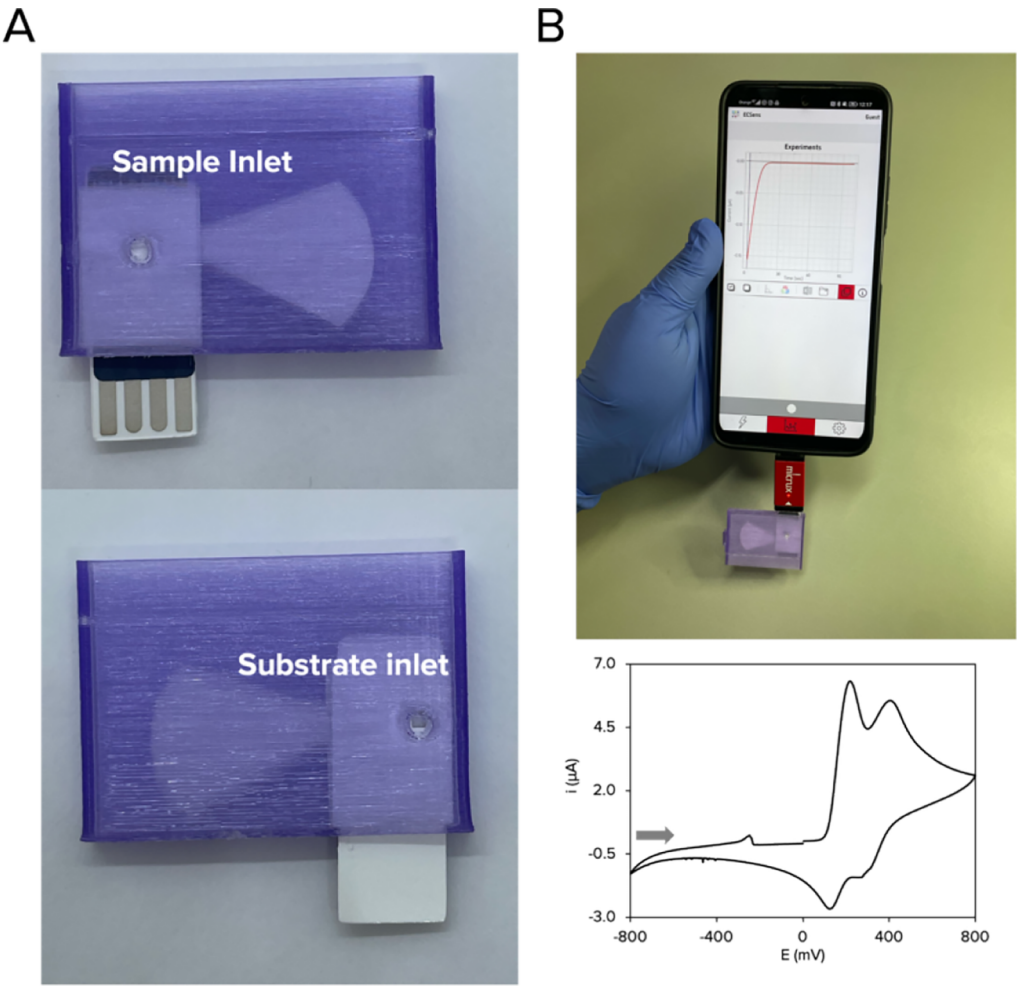


Figure 4. Toward a decentralized and user-friendly use of the eVFIA. (A) eVFIA within its 3D-printed case. (Top) Front view; (bottom) back view. (B) Decentralized setup for measurements outside the laboratory. (Bottom) CV of TMB solution recorded using the eVFIA and the USB-C potentiostat. Scan rate: 100 mV/s.

in the context of stroke diagnosis, where early detection of biomarkers such as GFAP can significantly impact clinical outcomes, as this biomarker is strongly correlated with stroke subtype and thus with different treatments. Rapid screening outside hospital environments could accelerate triage decisions and improve access to neuroprotective interventions.

■ CONCLUSIONS

Here, a multilayer paper-based architecture is assembled using a screen-printed electrochemical cell as both a physical support and transducer for creating an electrochemical vertical flow immunoassay (eVFIA). This device allows, after running an optimized sandwich immunoassay, sensitive electrochemical detection of GFAP in 10 min from sample addition to readout. The eVFIA for the rapid and quantitative determination of GFAP here presented provides important advantages over traditional flow assays. The vertical flow configuration improved sample distribution and reduced assay time compared to conventional lateral flow devices, while electrochemical readout provided robust quantitative signals independent of optical interferences. Systematic optimization of assay conditions, including antibody concentrations and incubation parameters, yielded good analytical performance, with results for clinical serum samples that showed good correlation with ELISA immunoassay in well plate.

The GFAP eVFIA addresses several limitations of current stroke biomarker determination by offering a low-cost, portable, and user-friendly alternative suitable for decentralized and prehospital settings. This capability is particularly relevant in time-critical stroke management, where rapid differentiation of stroke subtype can significantly influence treatment decisions and patient outcomes. The platform thus represents a promising complement to existing imaging-based methods and could be integrated into point-of-care diagnostic workflows.

However, while the assay demonstrated overall good performance, future work should explore improvements in its performance, widening the linear range of the assay, exploring the incorporation of a washing step after TMB incubation to potentially reduce background signal and enhance sensitivity, and automating sample dilution and substrate addition, as well as its adaptability to alternative sample types (e.g., plasma,[9] saliva[39] and, especially, nasal exudate[8]) for broader applicability. Furthermore, although the incorporation of dried reagents within the device favors storage and transportability, comprehensive stability studies should be done to support real-world deployment

Downloaded from http://pubs.acs.org/ascefj/article-pdf/doi/10.1021/acssensors.6c00801/65950242/se-2026-00801z.pdf by guest on 28 July 2026

https://doi.org/10.1021/acssensors.6c00801
ACS Sens. XXXX, XXX, XXX–XXX

and commercialization. Likewise, although reproducible performance was observed across different fabrication batches used throughout this work, dedicated large-scale batch-to-batch reproducibility studies will be required for clinical implementation.

Moreover, in the present work, the device is assembled manually to demonstrate proof-of-concept functionality and to allow rapid iterative optimization of the multilayer architecture. However, the fabrication steps could be fully compatible with established scalable manufacturing approaches used in paper-based and electrochemical devices. For example, layer patterning could be transferred to automated xurography, laser cutting, or roll-to-roll processing, while adhesive layers and functional pads could be prefabricated as die-cut components and aligned using registration fixtures. Automated dispensers could locate components sequentially over the polymeric film containing the screen-printed cells before cutting them. Therefore, the current manual assembly does not reflect a limitation of the concept but rather a prototyping stage that could be straightforwardly translated into automated production workflows.

In summary, the developed GFAP-eVFIA represents a significant advancement toward accessible, biomarker-based stroke diagnostics. With further refinement of the assay, simplification of its use (e.g., automation of sample/substrate addition) and large-scale clinical validation, this technology holds strong potential for deployment in emergency medical services, mobile stroke units, and other resource-limited healthcare settings, bridging the gap between laboratory-based diagnostics and true point-of-care stroke assessment.

■ ASSOCIATED CONTENT

Supporting Information

The Supporting Information is available free of charge at https://pubs.acs.org/doi/10.1021/acssensors.6c00801.

Additional experimental information and results (DOCX)

Supplementary Video (MP4)

■ AUTHOR INFORMATION

Corresponding Authors

Estefanía Costa-Rama – *Department of Physical and Analytical Chemistry, Universidad de Oviedo, Oviedo 33006, Spain; Biomedical Engineering Center, Universidad de Oviedo, Oviedo 33011, Spain;* orcid.org/0000-0002-5357-9269; Email: costaestefania@uniovi.es

M. Teresa Fernández-Abedul – *Department of Physical and Analytical Chemistry, Universidad de Oviedo, Oviedo 33006, Spain; Biomedical Engineering Center, Universidad de Oviedo, Oviedo 33011, Spain;* orcid.org/0000-0003-3782-5025; Email: mtfernandeza@uniovi.es

Authors

Pablo Rioboó-Legaspi – *Department of Physical and Analytical Chemistry, Universidad de Oviedo, Oviedo 33006, Spain;* orcid.org/0000-0001-6222-3937

Cristina Álvarez-Álvarez – *Department of Physical and Analytical Chemistry, Universidad de Oviedo, Oviedo 33006, Spain*

Ava Takenaka – *Department of Physical and Analytical Chemistry, Universidad de Oviedo, Oviedo 33006, Spain; Department of Biomedical Engineering, Texas A&M University, College Station, Texas 77843, United States*

Jad Wardeh – *Department of Physical and Analytical Chemistry, Universidad de Oviedo, Oviedo 33006, Spain; Department of Biomedical Engineering, Texas A&M University, College Station, Texas 77843, United States*

Carmen García-Cabo – *Department of Neurology, Hospital Universitario Central de Asturias, Oviedo 33011, Spain*

Lorena Benavente-Fernández – *Department of Neurology, Hospital Universitario Central de Asturias, Oviedo 33011, Spain*

Sergio Calleja-Puerta – *Department of Neurology, Hospital Universitario Central de Asturias, Oviedo 33011, Spain*

Complete contact information is available at: https://pubs.acs.org/doi/10.1021/acssensors.6c00801

Author Contributions

P.R.-L: Conceptualization, Methodology, Formal Analysis, Investigation, Visualization, Writing - Original Draft. C.A.-A: Methodology, Investigation, Formal Analysis, Visualization; A.T: Methodology, Investigation. J.W: Methodology, Investigation. C.G.-C: Resources, Methodology, Funding acquisition. L.B.-F: Resources, Methodology. S.C.-P: Resources, Methodology. E.C.-R: Conceptualization, Methodology, Writing-Review & Editing, Supervision, Project administration, Funding acquisition. M.T.F.-A: Conceptualization, Methodology, Writing-Review & Editing, Supervision, Project administration, Funding acquisition.

Notes

The data that support the findings of this work are available at the Repository of the University of Oviedo(RUO) at the URL: https://hdl.handle.net/10651/84952, with the following DOI: 10.17811/ruo_datasets.84952

The authors declare the following competing financial interest(s): M.T.F.-A. is one of the founders of Micrux Technologies, a company engaged in the development of miniaturized electrodes and electrochemical/microfluidic equipment and remains a consultant and shareholder. She declares it has not influenced the work reported in this paper. The rest of authors declare that the reported experimental results are not influenced by competing financial interests or personal relationships.

■ ACKNOWLEDGMENTS

This work has been supported by I+D+i project PID2023-148375OB-I00 funded by MCIU/AEI/10.13039/501100011033/FEDER, UE, and the Government of the Principality of Asturias through the Sekuens Agency, and EU through the FEDER Program (IDE/2024/000694). P.R.L. acknowledges support from the Asturian Council for Science, Technology, and Innovation ("Severo Ochoa" grant BP21-029).

■ REFERENCES

(1) Salvadori, E.; Papi, G.; Insalata, G.; Rinnoci, V.; Donnini, I.; Martini, M.; Falsini, C.; Hakiki, B.; Romoli, A.; Barbato, C.; Polcaro, P.; Casamorata, F.; Macchi, C.; Cecchi, F.; Poggesi, A. Comparison between Ischemic and Hemorrhagic Strokes in Functional Outcome at Discharge from an Intensive Rehabilitation Hospital. *Diagnostics* **2021**, *11* (1), 38.

(2) Kuriakose, D.; Xiao, Z. Pathophysiology and Treatment of Stroke: Present Status and Future Perspectives. *Int. J. Mol. Sci.* **2020**, *21* (20), 7609.

Downloaded from http://pubs.acs.org/ascefj/article-pdf/doi/10.1021/acssensors.6c00801/65950242/se-2026-00801z.pdf by guest on 28 July 2026

(3) Patil, S.; Rossi, R.; Jabrah, D.; Doyle, K. Detection, Diagnosis and Treatment of Acute Ischemic Stroke: Current and Future Perspectives. *Front. Med. Technol.* **2022**, *4*, No. 748949.
(4) Navi, B. B.; Audebert, H. J.; Alexandrov, A. W.; Cadilhac, D. A.; Grotta, J. C. Mobile Stroke Units: Evidence, Gaps, and Next Steps. *Stroke* **2022**, *53* (6), 2103−2113.
(5) Mattila, O. S.; Ashton, N. J.; Blennow, K.; Zetterberg, H.; Harve-Rytsälä, H.; Pihlasviita, S.; Ritvonen, J.; Sibolt, G.; Nukarinen, T.; Curtze, S.; Strbian, D.; Pystynen, M.; Tatlisumak, T.; Kuisma, M.; Lindsberg, P. J. Ultra-Early Differential Diagnosis of Acute Cerebral Ischemia and Hemorrhagic Stroke by Measuring the Prehospital Release Rate of GFAP. *Clin. Chem.* **2021**, *67* (10), 1361−1372.
(6) Jæger, H. S.; Tranberg, D.; Larsen, K.; Valentin, J. B.; Blauenfeldt, R. A.; Luger, S.; Bache, K. G.; Gude, M. F. Diagnostic Performance of Glial Fibrillary Acidic Protein and Prehospital Stroke Scale for Identification of Stroke and Stroke Subtypes in an Unselected Patient Cohort with Symptom Onset < 4.5 h. *Scand. J. Trauma Resusc. Emerg. Med.* **2023**, *31* (1), 1−11.
(7) Katsanos, A. H.; Makris, K.; Stefani, D.; Koniari, K.; Gialouri, E.; Lelekis, M.; Chondrogianni, M.; Zompola, C.; Dardiotis, E.; Rizos, I.; Parissis, J.; Boutati, E.; Voumvourakis, K.; Tsivgoulis, G. Plasma Glial Fibrillary Acidic Protein in the Differential Diagnosis of Intracerebral Hemorrhage. *Stroke* **2017**, *48* (9), 2586−2588.
(8) García-Cabo, C.; Rioboó-Legaspi, P.; Benavente-Fernández, L.; Costa-Rama, E.; Fernández-Abedul, M. T.; Calleja-Puerta, S. Measurement of GFAP in Nasal Exudate in the Differential Diagnosis between Ischemic Stroke and Intracerebral Hemorrhage. *Cerebrovasc. Dis.* **2024**, *53* (5), 515−518.
(9) Arslan, B.; Andreasson, U.; Rembeza, E.; Axelsson, M.; Novakova, L.; Kirsebom, B. E.; Fladby, T.; Dittrich, A.; Kern, S.; Skoog, I.; Blennow, K.; Zetterberg, H.; Kvartsberg, H. Validation of a Plasma GFAP Immunoassay and Establishment of Age-Related Reference Values: Bridging Analytical Performance and Routine Implementation. *Clin. Chem. Lab. Med.* **2025**, *63* (12), 2522−2535.
(10) Menéndez-Valladares, P.; M. Delgado, R.; Núñez-Jurado, D.; Sempere-Bordes, L.; Penalba, A.; Azurmendi, L.; Parolo, C.; Barragán, A.; Cabezas, J. A.; de Jesús Gil, C.; Moreno, J.; Canto Neguillo, R.; Valverde de Moyano, R.; García Garmendia, J. L.; García Murillo, M.; Muñoz Martínez, I.; Romero Hidalgo, A.; Aranda Aguilar, F.; Pérez Sánchez, S.; Sánchez, J. C.; Montaner, J. Smartphone-Enabled Point-of-Care Testing for Prehospital Stroke Diagnosis. *Prehosp. Emerg. Care* **2024**, *30*, 111.
(11) Harpaz, D.; Eltzov, E.; Seet, R. C. S.; Marks, R. S.; Tok, A. I. Y. Point-of-Care-Testing in Acute Stroke Management: An Unmet Need Ripe for Technological Harvest. *Biosensors* **2017**, *7* (3), 30.
(12) Ozcelikay, G.; Mollarasouli, F.; Unal, M. A.; Gucuyener, K.; Ozkan, S. A. Ultrasensitive Determination of Glial-Fibrillary-Acidic-Protein (GFAP) in Human Serum-Matrix with a Label-Free Impedimetric Immunosensor.*Biosensors* **2022**, *12* (12), 1165.
(13) Khetani, S.; Salahandish, R.; Tabor, J. B.; Chilvers, M.; Dukelow, S.; Ho, C.; Campbell, C.; Sen, A.; Debert, C. T.; Sanati-Nezhad, A. Nanoporous Carbon Immunosensor for Highly Accurate and Sensitive Clinical Detection of Glial Fibrillary Acidic Protein in Traumatic Brain Injury, Stroke, and Spinal Cord Injury. *ACS Biomater. Sci. Eng.* **2023**, *9* (6), 3556−3569.
(14) Wang, T.; Fang, Y.; He, Z. Electrochemical Quantitative Detection of Glial Fibrillary Acidic Protein Based on Molecularly Imprinted Polymer Sensor. *Int. J. Electrochem. Sci.* **2017**, *12* (8), 7341−7350.
(15) Krausz, A. D.; Korley, F. K.; Burns, M. A. The Current State of Traumatic Brain Injury Biomarker Measurement Methods. *Biosensors (Basel)* **2021**, *11* (9), 319.
(16) Middleton, J. UCH-L1 and GFAP Testing (i-STAT TBI Plasma) for the Detection of Intracranial Injury Following Mild Traumatic Brain Injury. *Am. Fam. Physician* **2022**, *105* (3), 313−314.
(17) Pedreira-Rincón, J.; Rivas, L.; Comenge, J.; Skouridou, V.; Camprubí-Ferrer, D.; Muñoz, J.; O'Sullivan, C. K.; Chamorro-Garcia, A.; Parolo, C. A Comprehensive Review of Competitive Lateral Flow Assays over the Past Decade. *Lab Chip* **2025**, *25* (11), 2578−2608.
(18) Di Nardo, F.; Chiarello, M.; Cavalera, S.; Baggiani, C.; Anfossi, L. Ten Years of Lateral Flow Immunoassay Technique Applications: Trends, Challenges and Future Perspectives. *Sensors* **2021**, *21* (15), 5185.
(19) Abarintos, V.; Piper, A.; Merkoci, A. Electrochemical Lateral Flow Assays: A New Frontier for Rapid and Quantitative Biosensing. *Curr. Opin. Electrochem.* **2025**, *54* (12), No. 101750.
(20) Nandhakumar, P.; Muñoz San Martín, C.; Arévalo, B.; Ding, S.; Lunker, M.; Vargas, E.; Djassemi, O.; Campuzano, S.; Wang, J. Redox Cycling Amplified Electrochemical Lateral-Flow Immunoassay: Toward Decentralized Sensitive Insulin Detection. *ACS Sens.* **2023**, *8* (10), 3892−3901.
(21) Gonzalez-Macia, L.; Li, Y.; Zhang, K.; Nunez-Bajo, E.; Barandun, G.; Cotur, Y.; Asfour, T.; Olenik, S.; Coatsworth, P.; Herrington, J.; Güder, F. NFC-Enabled Potentiostat and Nitrocellulose-Based Metal Electrodes for Electrochemical Lateral Flow Assay. *Biosens. Bioelectron.* **2024**, *251* (10), No. 116124.
(22) Ying, X.; Fu, W.; Zhu, L.; Sun, T.; Qi, M.; Zhou, L.; Wang, Y.; Wang, J.; Su, B.; Zhang, J. Electrochemical Lateral Flow Immunoassay with Built-In Electrodes for Ultrasensitive and Wireless Detection of Inflammatory Biomarkers. *Anal. Chem.* **2024**, *96* (26), 10630−10638.
(23) Núnez-Bajo, E.; Carmen Blanco-López, M.; Costa-García, A.; Teresa Fernández-Abedul, M. Integration of Gold-Sputtered Electrofluidic Paper on Wire-Included Analytical Platforms for Glucose Biosensing. *Biosens. Bioelectron.* **2017**, *91*, 824−832.
(24) Lee, M.; Rafiq Sayyed, D.; Kim, H.; Sanchez, J. C.; Sik Hong, S.; Choi, S.; Kim, H.; Han, E.; Won Kang, H.; Min Kim, J.; Joan, M.; Kim, H.; Chae, H.; Park, J. M. A Comprehensive Exdia TRF-LFIA for Simultaneous Quantification of GFAP and NT-ProBNP in Distinguishing Ischemic and Hemorrhagic Stroke. *Clin. Chim. Acta* **2024**, *557* (6), No. 117872.
(25) Sun, J.; Gao, F.; Song, Y.; Wang, M.; Wang, C.; Ni, Q.; Wang, Y.; Yang, M.; Zhao, P.; Sun, B. Paper Lateral Flow Strips Based on Gold Nanorods for Ultrasensitive Detection of Traumatic Brain Injury Biomarkers. *ACS Appl. Nano Mater.* **2023**, *6* (20), 18729−18738.
(26) Kaur, M.; Eltzov, E. Optimizing Effective Parameters to Enhance the Sensitivity of Vertical Flow Assay for Detection of Escherichia Coli. *Biosensors* **2022**, *12* (2), 63.
(27) Jeon, J.; Choi, H.; Han, G. R.; Ghosh, R.; Palanisamy, B.; Di Carlo, D.; Ozcan, A.; Park, S. Paper-Based Vertical Flow Assays for in Vitro Diagnostics and Environmental Monitoring. *ACS Sens.* **2025**, *10* (5), 3317−3339.
(28) Traipop, S.; Jampasa, S.; Tangkijvanich, P.; Chuaypen, N.; Chailapakul, O. Dual-Label Vertical Flow-Based Electrochemical Immunosensor for Rapid and Simultaneous Detection of Hepatitis B Surface and e Virus Antigens. *Sens. Actuators, B* **2023**, *387*, No. 133769.
(29) Ying, X.; Fu, W.; Qi, M.; Zhou, L.; Li, W.; Su, B. Ultrasensitive Electrochemical Vertical Flow Immunoassay for Rapid and Simultaneous Detection of Interleukin-6 and Procalcitonin. *ACS Sens.* **2024**, *9* (12), 6667−6674.
(30) Mohd, O.; Sotoudegan, M. S.; Ligler, F. S.; Walker, G. M. A Simple Cantilever System for Measurement of Flow Rates in Paper Microfluidic Devices. *Engineering Research Express* **2019**, *1* (2), No. 025019.
(31) Bahadır, E. B.; Sezgintürk, M. K. Lateral Flow Assays: Principles, Designs and Labels. *TrAC, Trends Anal. Chem.* **2016**, *82*, 286−306.
(32) Parolo, C.; de la Escosura-Muñiz, A.; Merkoçi, A. Enhanced Lateral Flow Immunoassay Using Gold Nanoparticles Loaded with Enzymes. *Biosens. Bioelectron.* **2013**, *40* (1), 412−416.
(33) Lukyanov, A. V.; Mitkin, V. V.; Pryer, T.; Sirimark, P.; Theofanous, T. G. Capillary Transport in Paper Porous Materials at Low Saturation Levels: Normal, Fast or Superfast?. *Proc. Math. Phys. Eng. Sci.* **2020**, *476* (2244), No. 20200488.
(34) Yetisen, A. K.; Akram, M. S.; Lowe, C. R. Paper-Based Microfluidic Point-of-Care Diagnostic Devices. *Lab Chip* **2013**, *13* (12), 2210−2251.
(35) Moreno, E.; Kumar, P.; Adansi, R. O.; Rodriguez, A.; Kumar, V. Exploring Capillary Flow in Paper-Based Microfluidics: Unraveling

Downloaded from http://pubs.acs.org/ascefj/article-pdf/doi/10.1021/acssensors.6c00801/65950242/se-2026-00801z.pdf by guest on 28 July 2026

Mechanics and Applications. In *Fluids engineering division summer meeting*; American Society of Mechanical Engineers, **2024**, *2*, pp V002T06A004.
(36) Abedsoltan, H. A Review on Liquid Flow through Low-Density Fibrous Porous Media. *Chem. Eng. Res. Des.* **2023**, *200*, 445−455.
(37) Amalia, L. Glial Fibrillary Acidic Protein (GFAP): Neuroinflammation Biomarker in Acute Ischemic Stroke. *J. Inflamm. Res.* **2021**, *14*, 7501−7506.
(38) Paul, J. F.; Ducroux, C.; Correia, P.; Daigneault, A.; Larochelle, C.; Stapf, C.; Gioia, L. C. Serum Glial Fibrillary Acidic Protein in Acute Stroke: Feasibility to Determine Stroke-Type, Timeline and Tissue-Impact. *Front. Neurol.* **2024**, *15*, No. 1470718.
(39) Katsipis, G.; Tzekaki, E. E.; Tsolaki, M.; Pantazaki, A. A. Salivary GFAP as a Potential Biomarker for Diagnosis of Mild Cognitive Impairment and Alzheimer's Disease and Its Correlation with Neuroinflammation and Apoptosis. *J. Neuroimmunol.* **2021**, *361*, No. 577744.
(40) Emmerich, J.; Chanpura, A.; Lu, T.; Baird, A.; Barone, F.; Gustafson, D.; Siepmann, T.; Huttner, H.; Barlinn, K. Blood-Based MMP-9 for the Early Differentiation of Acute Ischemic Stroke: A Systematic Review and Meta-Analysis. *J. Stroke Cerebrovasc. Dis.* **2025**, *34* (11), No. 108454.
(41) Rezaei, O.; Pakdaman, H.; Gharehgozli, K.; Simani, L.; Vahedian-Azimi, A.; Asaadi, S.; Sahraei, Z.; Hajiesmaeili, M. S100 B: A New Concept in Neurocritical Care. *Iran. J. Neurol.* **2017**, *16* (2), 83.

Downloaded from http://pubs.acs.org/ascefj/article-pdf/doi/10.1021/acssensors.6c00801/65950242/se-2026-00801z.pdf by guest on 28 July 2026

https://doi.org/10.1021/acssensors.6c00801
ACS Sens. XXXX, XXX, XXX−XXX